Expanding sample volume for microscopical detection of nanoplastics

Arto Hiltunen,[a*] Joona Huopalainen,[b] Ermei Mäkilä,[c] Sirkku Häkkilä,[d] Pia Damlin,[b] Jari Hänninen[a]

March 25, 2024

[a] Archipelago Research Institute, Biodiversity Unit of the University of Turku, 20014, Finland
[b] Materials Chemistry Research Group, Department of Chemistry, University of Turku, 20014 Turku, Finland
[c] Department of Physics and Astronomy, University of Turku, 20014, Finland
[d] Laboratory of Aerobiology, Biodiversity Unit of the University of Turku, 20014, Finland
[*] Corresponding author: arto.hiltunen@utu.fi

Abstract

The extent of nanoplastic pollution has raised severe environmental and health concerns. While the means for microplastic detection are abundant, improved tools for nanoplastic detection are called-for. State-of-the-art microscopic techniques can detect nanoplastics down to tens of nanometers, however, only from small sample sizes (typically ~ 10 µl). In this work, we describe a method that enables sampling of 1 liter of seawater by the means of correlative Raman- and SEM-techniques. This is achieved by adapting common microplastic sample purification protocols to suit the nanoplastic study. In addition, we decorate a membrane filter with SERS-property to amplify the Raman signals. Together, the purification method combined with the use of the SERS-activated-membrane-filter enables identification and imaging of individual nanoplastic particles from significantly larger sample sizes than before. In the nanoscale the average recovery rate is 5 %. These results aim to provide useful tools for researchers in the fight against plastic pollution.

Keywords: nanoplastic, chemical digestion, seawater, electron microscopy, Raman microscopy, SERS

1 Introduction

It has been estimated that 60 % of all plastics ever made, has been discarded either in the landfills or in the environment.[1] This has caused a global littering problem which was acknowledged in scientific literature already 50 years ago.[2,3] What makes the plastic waste problem especially challenging to manage is the breakage of the plastic materials into small pieces called micro- and nanoplastics, depending on how small they are. In this paper, we use the convention to call 5 mm - 1 µm plastic particles as microplastics and 1 - 999 nm particles as nanoplastics. The breakage is thought to be caused by mechanical abrasion, UV-light, or digestion by small animals.[4–7] Moreover, the most recent research shows that even brand new plastic products release large numbers of small plastic particles during usage (e.g. infant drinking bottles or tea bags).[8,9] Hence, small plastic particles from whichever aforementioned origin, are now found on land, at sea, and in the air, even in the most remote places on Earth, down to sediments dated back to the 18th century.[10–14]

While the harm from large plastic pieces to humans is mainly aesthetic (e.g. trashing of beaches) the micro- and nanoplastics have raised a health concern.[15] Owing to their small size micro- and nanoplastics can enter the human body: Ragusa et al. reported microplastics in human placentas and Leslie et al. reported microplastics and nanoplastics in blood.[16,17] In general, it is thought that particles smaller than 1 micrometer may enter cells and particles smaller than 200 nm may cross the blood-brain barrier raising concern that the plastic might reach the brain.[15]

The methods to study microplastics are well established, however the means to study nanoplastics are still incomplete. According to a recent review, nanoplastics are in most cases detected using pyrolysis coupled to gas chromatography-mass spectrometry (Py-GC-MS).[18] While the Py-GC-MS has proven to be extremely useful tool, and provided us with the first estimations on the nanoplastic concentration (µg/l) in various different environments, the shortfall of the method is that it cannot provide the particle count nor the size distribution in the sample. As, for example, the particle size determines how deep in the body they can travel, it is of utmost importance to have data on the particle counts down to the nanosize. Very recently, Bauten et al. reported a promising way to use flow cytometry to count nanoplastics using polymer binding peptides, but the application to environmental samples is yet to be demonstrated.[19]

Raman microscopy has been shown to be an efficient technique to detect nanoplastics. Many groups have developed methods to find nanoplastics using Raman from within relatively clean sample matrices which do not require purification such as tap water or ultrapure water (e.g. Milli-Q).[20–24] In addition to Raman, microscopic images have been obtained from clean matrices using SEM combined with XPS and FTIR[8] or STXM and NEXAFS combined with TEM.[25] In contrast to ultrapure water, environmental samples are more complicated to analyze (e.g. sea or lake water) due to vast amount of organic and inorganic matter present in the sample relative to the targeted plastics. Despite the challenging matrix, recent literature describes success in nanoplastic detec-

tion from natural waters using Raman techniques, namely, Raman tweezers,[26] and SERS (Surface Enhanced Raman Spectroscopy).[27–29] However, the sample size so far has remained low, being typically 10 µl or "a drop" of unconcentrated and unpurified water. If the sample is not purified (i.e. not chemically digested) it will hamper the nanoplastic analysis, in particular, when using microscopic methods. Firstly, the small nanosized plastic particles might get buried under the organic matter making it impossible to image them. Secondly, identifying the plastics based on their Raman spectrum will be complicated as well due to background fluorescence signal from the organic matter. In fact, several authors have acknowledged the problem caused by the background signal when working with unpurified samples.[27,28,30,31] Moreover, to utilize SERS effectively, the examined nanoplastics must be within a few nanometers of the metal surface.[32] Therefore the nanoplastic particle under investigation should ideally lie on the surface of the SERS-substrate without any matter in between.

The lack of a suitable purification protocol designed for microscopic investigation of complex sample matrices is essentially limiting the sample size to a drop. Concentrating a larger sample would also concentrate the organic and inorganic matter which would then bury the small nanoplastics making the use of microscopic methods impossible. To solve this problem, in this work, we show how to purify 1 liter of seawater to such detail that individual nanoplastic particles can be identified using Raman spectroscopy and high magnification images obtained using scanning electron microscopy (FESEM). To assist in the detection of nanoplastics, a SERS-activated-membrane-filter is used to filter out the final reagent allowing direct observation of the particles from this very same filter. As far as we know, this is the first demonstration of reaching nanoscale resolution using microscopic techniques from such large sample size of actual seawater.

2 Materials and Methods

2.1 Sampling and storing of seawater

Seawater samples were collected from the Baltic Sea at Ispoinen Beach (60°24'52"N 22°15'33"E) on 3.10.2022 and Kansanpuisto Beach (60°25'35"N 22°10'59"E) on 14.2.2023 both locating in the coast of Turku, Finland. Sampling was done by filling 5 l glass bottles with surface water at the sampling sites. Filled bottles were closed with ground joint glass stopper and covered with a piece of aluminium foil to protect the sample from contamination as shown in the photograph in Figure 4. The samples were stored at 3 °C in dark until further processing. During the storing, matter denser than water (e.g. sand) sank to bottom of the sampling bottle.

2.2 Chemicals for sample matrix digestion

Hydrogen peroxide (H_2O_2, 30 % analytical reagent grade) was supplied from Fischer Scientific. Hydrochloric acid (HCl, 37 %, analytical reagent grade) and sodium hydroxide (NaOH, pellets, 98.9 %) were supplied from VWR. NaOH pellets were dissolved in Milli-Q water to achieve 0.1 M NaOH solution. HCl was diluted with Milli-Q water to achieve 10 % HCl solution. All these chemicals were filtered through polyethersulfone (PES) membrane filter (Sartorius Type 15407, 0.2 µm pore size, 47 mm diameter) prior use.

2.3 The chemical digestion protocol

1 l of seawater (Ispoinen Beach) from the 5 l sampling bottle was carefully poured into a large flask trying to leave the sand behind. Next, the seawater was poured onto a polycarbonate (PC) filter, and suction filtered. Residue left on the filter was collected by transferring the filter into round-bottom flask. The leftover filtrate was discarded. For the first digestion step, 30 ml of 30 % H_2O_2 was added into the flask. A recovery bend was added to the flask to serve as a cap to minimize the risk of contamination but simultaneously allowing gases to evaporate freely (also applied in the further steps). The filter was bathed in the H_2O_2 for a week. During this time, the flask was at 50 °C water bath for 3 consecutive days 6 h/day (on 2nd, 3rd and 4th day). In the morning of each day of heating, 10 ml of 30 % H_2O_2 was added into the flask. Rest of the time the flask was kept at room temperature.

After the week, the sample in H_2O_2 was poured onto a new PC filter and suction filtered. The flask (where the first filter still remains) was rinsed with 30 ml of Milli-Q water for 6 times to collect all particles. The rinsing water was poured onto the new PC filter and suction filtered. Next the new filter was moved into clean round-bottom flask where 30 ml of 0.1 M NaOH was added. The sample was digested in NaOH for 24 h at room temperature.

After the 24 h, the sample in NaOH was poured onto a new PC filter, and suction filtered. The flask was rinsed with 30 ml of Milli-Q water for 6 times. After the sample in NaOH and the rinsing Milli-Q water were suction filtered, the filter was moved into a round-bottom flask. 10 ml of 10 % HCl was added and let the digestion proceed for 1 h at room temperature. Finally, the HCl was removed by filtering the sample through a new PC filter.

A small piece (< 1 cm^2) of PC filter was cut every time before the filter was moved into the round-bottom flask, in order to image the processing steps (presented in Figure 1). These small pieces were taped onto pin mount specimen holders with carbon tape and sputtered with 10 nm of platinum prior SEM imaging.

2.4 SERS-activated-membrane-filter

Platinum (deposition thickness 12 nm) was sputtered onto Al_2O_3 membrane filters (Cytiva Whatman Anodisc Circle with Support Ring, 25 mm, 0.2 µm

pore size) using Quorum 150V ES+ sputter coater.

Spherical PS nanoparticles (Latex Microsphere Suspension, 10 % w/w, mean diameter 0.50 µm, Catalog Number 5050A) were purchased from Thermo Fisher Scientific. They were diluted 1000 times prior using (10 µl PS suspension to 10 ml Milli-Q water). Then 10 µl of the 1000x diluted PS suspension was pipetted into 30 ml of Milli-Q water, which was then filtered onto the Pt-coated (i.e. SERS-activated) or uncoated Al_2O_3 filters. After the filters had dried, they were characterized with Raman microscope.

2.5 In-house made polystyrene (PS) nanoparticles

The in-house made PS nanoparticle solution, was prepared as follows. Polystyrene packages from alimentary products were collected and washed with soap and water. Small amount of PS powder was prepared by sawing the packages with a hand saw. Next the powder was ground to nanosize using a ball mill the following way. Total of 1 g of white PS sawdust was added into 5 separate borosilicate glass vials (200 mg/each). 2 g of zirconium grinding beads (diameter: 1 mm) and 2 ml of ethanol were added into each vial. Vials were put into designated vial holder which was then attached into the planetary ball mill (Fritsch Pulverisette 7). Grinding duration and speed were chosen according to the study of El Hadri et al.[33] (speed: 450 rpm, duration: 40 cycles of 3 min of grinding and 6 min of pause). After the grinding, the top 1 ml of each vial was collected into a new vial (a photograph shown in Supporting Information Figure S1). PS concentration of the resulted solution was calculated by filtering 1 ml of the solution through a filter (pore size: 200 nm) and weighing the retentate resulting in 0.53 ± 0.08 mg/ml.

2.6 Demonstration with seawater-nanoplastic mixture

1 l of seawater (Kansanpuisto Beach) from the 5 l sampling bottle was carefully poured into a large flask to leave the sand behind. Next, 100 µl of in-house made PS nanoparticle solution was added into the same flask and mixed. The resulting plastic concentration became 53 ± 8 µg/l.

The water was treated as described above in section *The chemical digestion protocol* with the exception that the HCl was removed by filtering the sample through the Pt-coated Al_2O_3 filter (instead of a PC filter), which was designed to act as the SERS-substrate. Prior characterization with Raman microscope and SEM, the filter was let to dry at room temperature.

After the filter had dried, small scratch was done in the middle of the filter with injection needle to mark the (0,0)-coordinate point according to which the plastic particles were located.

All steps until here were performed in Class II-level biosafety cabinets to protect the samples from contamination.

Then the filter was characterized with Raman microscope, and the smallest plastics were targeted. Raman spectra of found nanoplastics were compared to a spectrum, which was obtained from the same white PS plastic, from which the

nanoplastics were made. Once a nanoplastic particle was found, its coordinates were noted down. Later, using the coordinates, the same PS nanoparticles were accurately found and high magnification images obtained with SEM.

2.7 Recovery rates calculation

The recovery rate was calculated by dividing the number of particles found in the sample filter by the number found in the reference filter and then multiplying the result by 100 %. In more detail, the maximum and minimum dimension from all the plastic particles in an area was measured (see Supporting Information Figure S2 for an example measurement). Based on the measurements, the number of particles was classified according to their sizes (100-200 nm, 200-300 nm,..., 900-1000 nm, 1-2 µm, 2-3 µm,..., 8-9 µm, > 10 µm). Then the recovery rate was calculated according to formula:

$$\text{Recovery rate}_i = \frac{\text{count}_i^{sample}/\text{area}^{sample}}{\text{count}_i^{ref}/\text{area}^{ref}} \cdot 100\%, \quad (1)$$

where i = 100-200 nm,..., 900-1000 nm, 1-2 µm,..., 8-9 µm, > 10µm, $count_i$ is the number of particles found corresponding to size range i, $area$ is the area from which the particles where counted, $sample$ refers to the sample under study, and ref refers to the reference sample where plastics are detected without losses.

The recovery rates presented in Figure 9 were calculated from a sample where 100 µl of nanoparticle solution was mixed with 1 liter of ultrapure water (Milli-Q) resulting in concentration of 53 ± 8 µg/l. The sample was processed as described above. As a reference sample the same amount of nanoparticle solution (100 µl) was directly pipetted onto the filter (Al_2O_3/Pt).

To calculate the recovery rates of particles up to 4 µm in size, 127 particles were found and measured on the sample filter from an area of 117 300 µm^2, while 427 particles were found in the examined area on the reference filter, which had an area of 27 600 µm^2.

Particles larger than 4 µm were counted from larger areas: 291 575 µm^2 and 219 528 µm^2 for sample and reference filter, respectively. The SEM image used in calculation (patched together from multiple smaller images) is presented in Supporting Information Figure S3. During the examination, 113 particles larger than 4 µm were found on the sample filter, while 191 particles were found in the examined area on the reference filter

2.8 Raman microscopy

The Raman instrument was Renishaw Qontor inVia Raman microscope equipped with Leica Microscope, a CCD detector and 1800 l/mm grating. Raman spectra were recorded at room temperature using 532 nm laser (RL532C50, Renishaw). The power of the laser was adjusted as high as possible without burning the PS spheres on the platinum coated filter (0.171 mW). The spectra were recorded

on single scan using 100 s acquisition time and 100x objective. Peaks caused by cosmic rays were removed from the data, and baseline correction was applied using the inVia. The spectra are shown without any smoothing.

2.9 Electron microscopy (FESEM/EDS)

Electron micrographs and elemental analysis of the samples were taken with Apreo S (Thermo Scientific, The Netherlands) field-emission SEM, equipped with Ultim Max 100 energy dispersive spectrometer (EDS; Oxford Instruments, UK). High magnification images were collected using an acceleration voltage of 2 kV. For confirming the composition of the samples, elemental maps and EDS spectra were acquired using an acceleration voltages of 4-6 kV. Compositional analysis was done using AZtec 6.1. software (Oxford Instruments).

3 Results and discussion

In this section we first introduce the chemical digestion protocol designed for nanoplastic research, and show how each reagent acts on the seawater sample. Next, we introduce the developed SERS-activated-membrane-filter and show how it amplifies the signals from small nanoplastics. Finally, we introduce the whole protocol by showing how the chemical digestion is used together with the SERS-activated-membrane-filter to find nanoplastic particles mixed with seawater.

3.1 The chemical digestion protocol

Common chemical digestion protocols for (micro)plastic extraction from complex matrices include the use of acids (HCl, H_2SO_4 or HNO_3) bases (KOH or NaOH) and oxidizers (H_2O_2 or Fenton reagent) with varying order, combination, concentration, processing times and temperatures.[34–36] Typically, in the last stage prior to microscopic examination the reagent is filtered out, sample is rinsed with water to remove reagent traces, and then analyzed. Based on existing literature on microplastics we have put together a chemical digestion protocol suitable for nanoplastics. From the multiple possibilities we optimized for digestion efficacy taking into account chemical compatibility of the filters and the reagent.

The digestion protocol was first tested with seawater without added nanoplastics in it, and the effect of each reagent was examined microscopically. Polycarbonate filters were used throughout as only the reagents' effects on the seawater components was examined, and therefore no SERS was needed.

We began by filtering 1 liter of seawater onto a 200 nm pore size polycarbonate filter. Due to rather large amount of organic matter in the Baltic sea the 200 nm filter pore size was selected to enable reasonable filtering time.

The first row in Figure 1 shows the retentate after filtering 1 liter of seawater without any purification. The filter surface is covered with bacteria, diatoms and

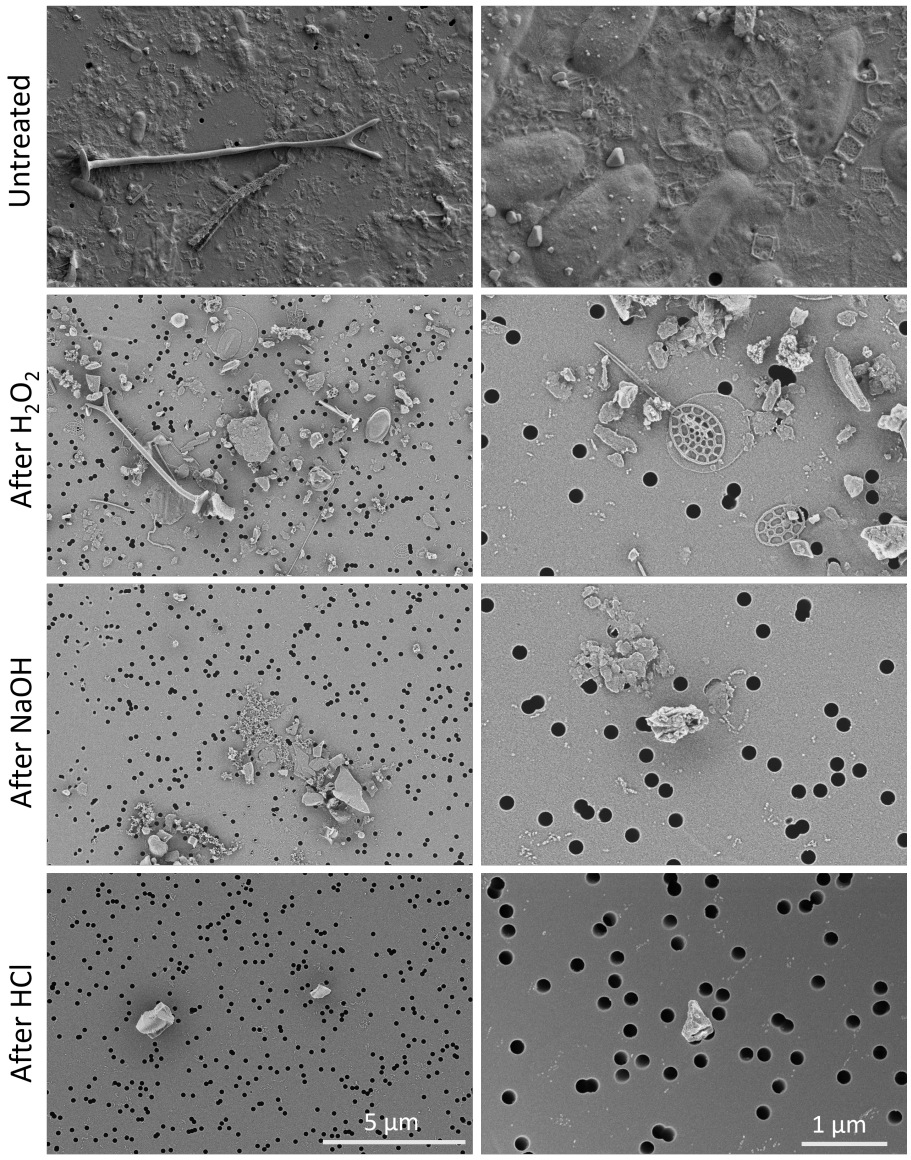

Figure 1: The figure shows the sequential effect of each digestion reagent on the sample. The first row shows the filter surface after 1 liter of seawater was filtered through it. In the last row the sample has been treated with H_2O_2, NaOH and HCl. Each column has the same magnification.

phytoplankton. Trying to distinguish individual nanosized plastics from within this matter that is several times larger (e.g. the length of bacteria is around 1-2 µm) would be extremely challenging. In addition, the organic matter can be

highly fluorescent which would disturb the Raman measurements. The images thus clearly show the need for an efficient purification protocol.

For the first digestion reagent we selected H_2O_2 and the result can be seen in the second row of Figure 1. The H_2O_2 has effectively removed all of the organic matter. Earlier literature suggests that other oxidizers, namely sodium hypochlorite (NaClO), would be more efficient than H_2O_2. However, in our experiments with the selected digestion time, temperature, added amount and concentration, we didn't see any residue of organic matter when using H_2O_2. Therefore, we concluded that for our purposes the H_2O_2 was efficient enough. After the H_2O_2 digestion, there appeared still to be a lot of inorganic matter left (e.g. diatoms) that could be further digested with other reagents. Diatoms' siliceous shells can't be digested using H_2O_2 but can be dissolved using NaOH.[37]

The result of NaOH digestion can be seen in 3rd row of Figure 1. The diatoms have been effectively removed and the filter surface has become again cleaner. It is worth noting that, polycarbonate has limited resistance against NaOH, however we found that the selected overnight reaction in 0.1 M NaOH effectively removed the diatoms without causing any damage to the filter that would be visible by eye or the electron microscope.

After NaOH, the sample matrix was digested using HCl in case there was calcareous ($CaCO_3$) items (e.g. minerals or mollusc shells) left in the sample. The end result of the process seems ideal for the nanoplastic detection using spectro-microscopic techniques: individual particles are against the clean surface of the filter without any fluorescent background present.

Milder purification conditions could be achieved using enzymatic digestion protocols which are performed in aqueous solutions in close to neutral pH (5-9).[38] Avoiding strong chemicals would also reduce the risk of damaging the plastics during the purification. However, we selected the chemicals and their strength such that they have been shown to have no or very little effect on the most common plastics according to literature.[34]

3.2 SERS-activated-membrane-filter

Typically when using Raman to detect nanoplastics, SERS is employed to get enough signal from the tiny particles. The SERS-effect can be created by depositing the sample on a nanostructured metal substrate or by the addition of nanoparticles onto the substrate or onto the sample. The signal enhancement is a result of laser excitation of the localized surface plasmon resonances (LSPR) which are located at the sharp features of the nanostructured surface.[39]

The SERS-function was generated onto alumina membrane filters (pore size 200 nm) via sputtering a thin layer of platinum onto the filters. Figure 2 shows that the platinum coating creates an even conformal coating without any damage or alteration of the filter structure. The insets show that upon coating, the white Al_2O_3 gets a darker coloring. The functioning as SERS-substrates was tested with 500 nm polystyrene spheres. Figure 3 shows a microscope image from both filter surfaces after a dispersion of polystyrene spheres was suction filtered through them. Next to the images, three representative Raman spec-

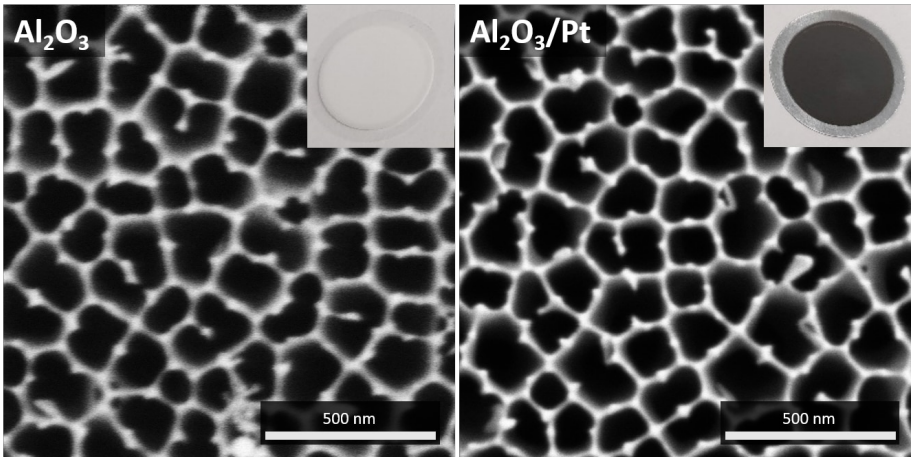

Figure 2: The figure shows scanning electron microscope images of an uncoated Al_2O_3 filter surface (left) and the SERS-active platinum coated Al_2O_3 filter surface (right). The insets show photographs of the same filters.

tra measured from the spheres retained on the filter surface are provided. The coating produces two enhancements. Firstly, the plastic particles become more visible against a colored background owing to the contrast difference (white plastic against dark filter) compared to the uncoated Al_2O_3 filter where the white particles disappear in the white background. Secondly, a clear enhancement of Raman signal intensity is observed on the coated filters. Measurement from the Al_2O_3 filter (uncoated) results in noisy and weak signals while on occasion a decent spectrum is recorded. The Pt-coated filter gives a clear signal repeatedly.

The problem of not being able to detect the particles from the microscope image is known and efforts have been made to improve their visibility. In the context of nanoplastic research, Yang et al.[40] reported that only particles larger than 500 nm could be optically resolved using their AgNW-based SERS-substrates, while Chang et al.[27] reported that only particles larger than 800 nm were visually detected using their nanowell SERS-substrates. Even when using commercial Klarite substrate as background, it has been reported that plastic particles below 1 µm are challenging to distinguish directly from the microscopic image.[30] In all these studies, rough surfaces were used as SERS-substrates, which can complicate the recognition of small particles. However, even against smooth surfaces, small plastic particles can be difficult to detect, if there is not enough contrast difference between the particles and the background. Oßmann et al.[41] reported that colorless 1 µm PS particles were difficult to detect against white PC membrane both under white light and dark-field illumination. In their work, the PS particles turned clearly visible only under dark-field illumination after they were deposited on to black or metal coated PC-membrane. Here, owing to the improved contrast between the Pt-coated

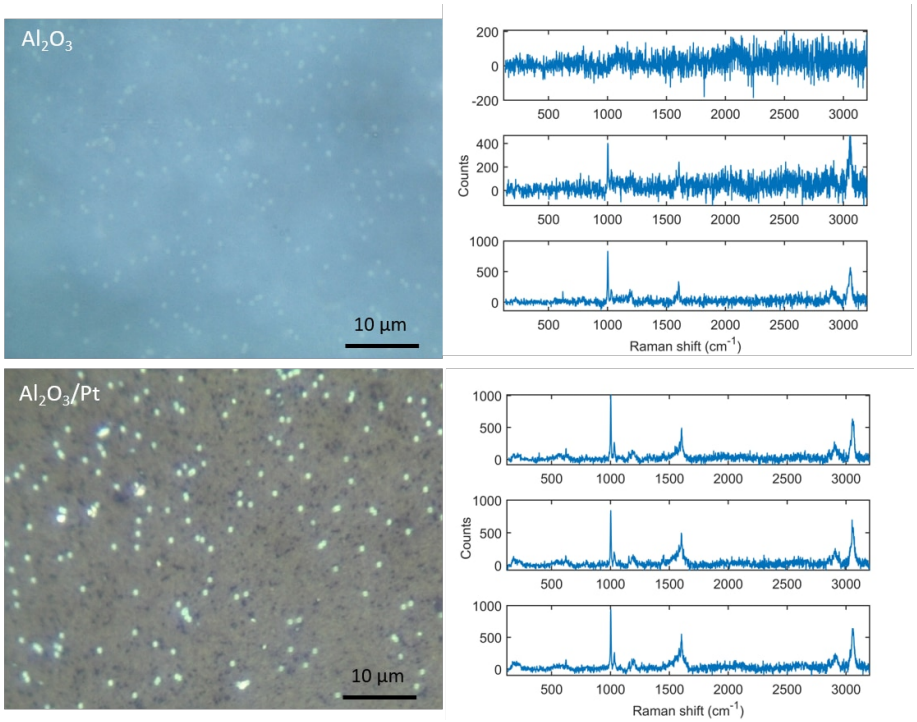

Figure 3: The left column shows microscope images from the 500 nm polystyrene nanoparticles on the tested filter surfaces: uncoated Al_2O_3 (above), and platinum coated Al_2O_3 (below). Next to the microscope images are three Raman spectra recorded from the polystyrene nanoparticles on that filter surface.

background, 500 nm PS spheres are easily detected from the Pt-coated filter surface under standard reflected white light illumination. As a result, the Raman spectra of individual nanoplastics can be acquired using point measurements thus no highly time-consuming Raman mapping is needed.

3.3 Demonstration with seawater-nanoplastic mixture

Next, the developed chemical digestion was used together with the SERS-activated-membrane-filter. The whole protocol is schematically shown in Figure 4. In brief, the seawater is filtered through a 200 nm pore size PC filter which is then digested in H_2O_2, NaOH, and HCl. The H_2O_2 and NaOH are filtered out using PC filters but the SERS-active Al_2O_3/Pt-filter is used to filter out the HCl, thus allowing for the imaging of nanoplastics directly from this filter.

The method was tested with a mixture of seawater and nanoplastics fabricated in the laboratory from consumer products according to Hadri et al.[33] We chose to test the method with environmentally relevant concentrations at 53±8 µg/l. This concentration falls within the reported range of nanoplastics con-

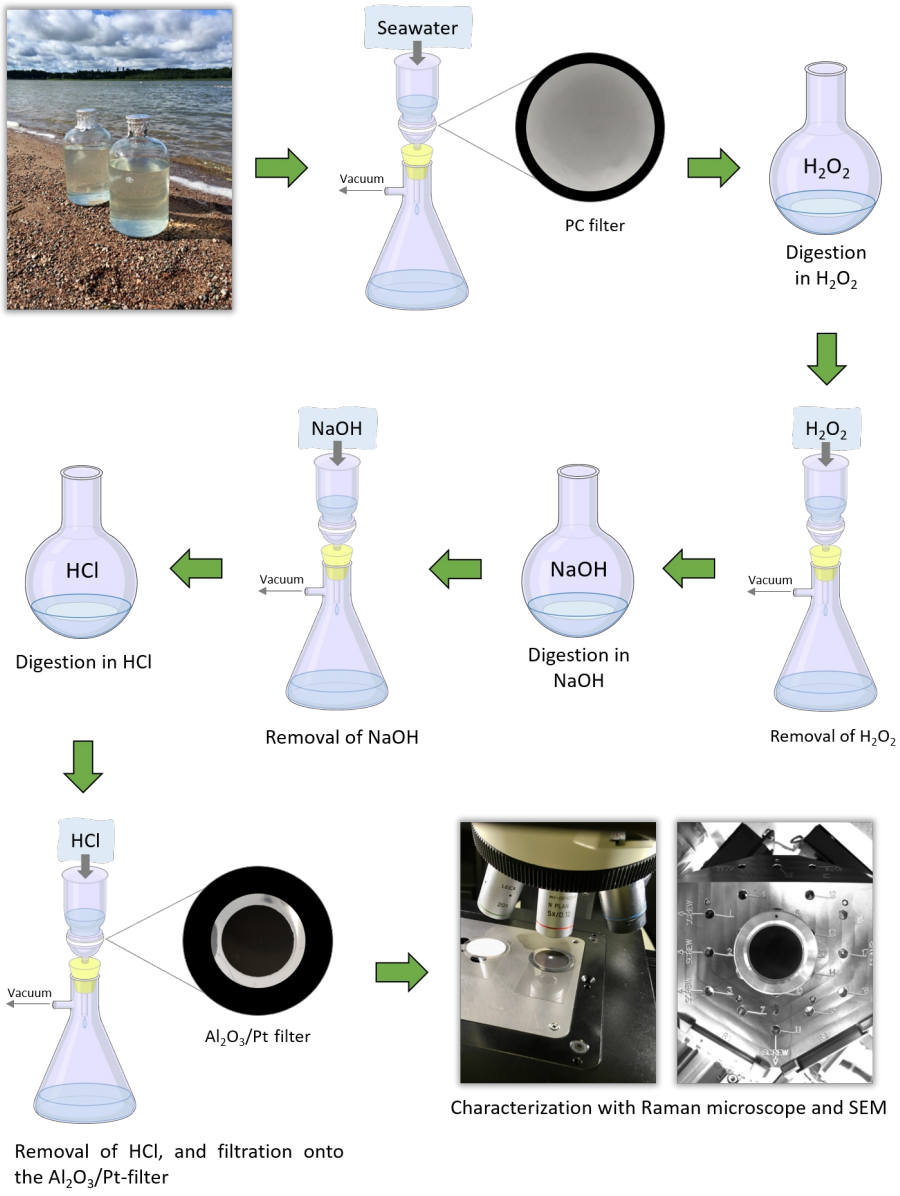

Figure 4: A scheme depicting the developed process for identifying and obtaining high magnification images from nanoplastics contained in seawater.

centrations in the environment, which can vary from 4.5 µg/l to 563 µg/l.[42,43] Figure 5 shows the Al_2O_3/Pt-filter surface after the plastic-seawater mixture has gone through the digestion protocol. Individual particles can be seen on

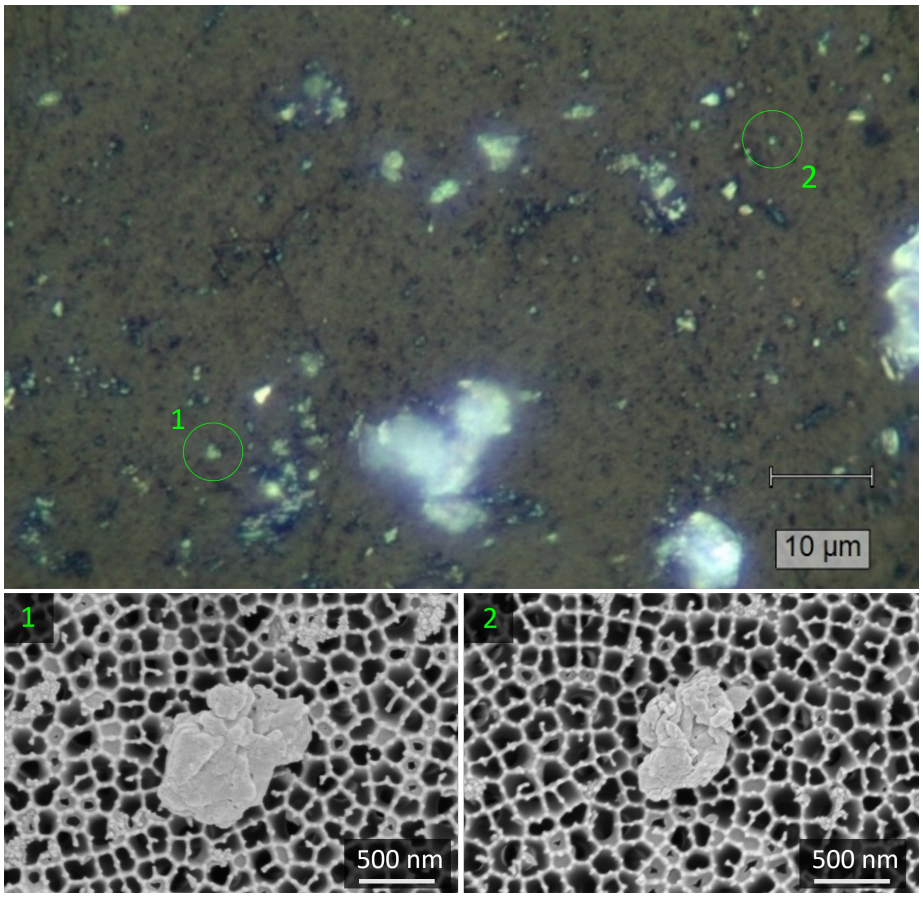

Figure 5: The optical microscope image (connected to Raman) above shows the plastics collected onto the Al_2O_3/Pt-filter surface after the sample was treated according to the developed protocol. The electron microscope images below show the smallest particles that were identified as polystyrene according to their Raman spectrum.

the filter surface and be tested whether they are plastic or not using Raman spectroscopy. Our digestion protocol has limitations, which will be discussed in more detail later. Consequently, other particles, such as sand, are also present on the filter surface. However, two smallest objects in this frame (Figure 5) that were identified as plastics based on their Raman spectrum (given in Figure 6) has been marked into the image. The spectra from the nanoplastics are in good accordance with spectrum measured from the original material from which the nanoplastics were prepared. It appears that the purification protocol does not damage or alter the chemical fingerprint of the nanoplastics. Moreover we haven't observed any alteration in the morphology of the nanoplastics after the

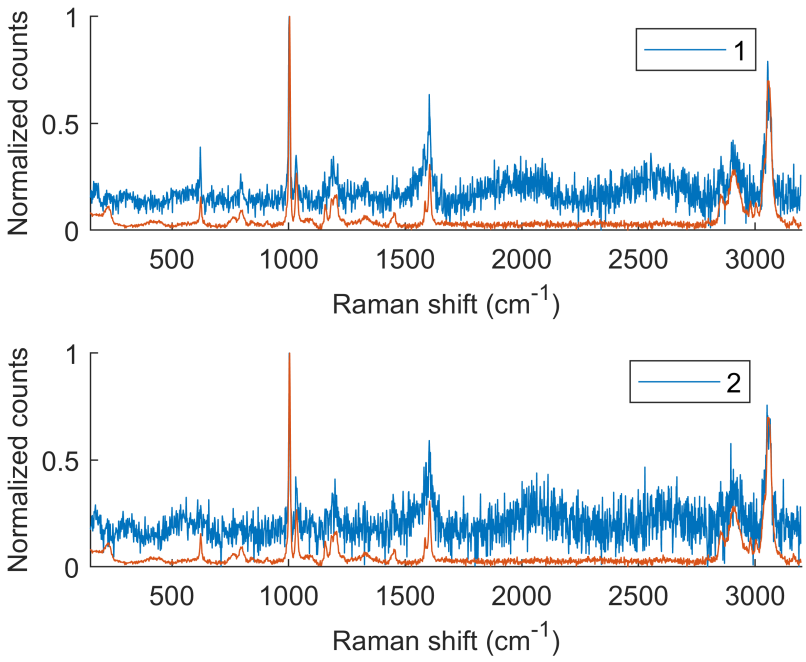

Figure 6: The figure shows Raman spectra (with blue) from particles 1 and 2 that were presented in Figure 5. The spectra are compared to a spectrum (with orange) that was recorded from the original large piece of plastic from which the nanoplastics were made.

processing compared to before processing (SEM images provided in Supporting Information Figure S4). Owing to sufficient purification, the objects could be identified using fast point measurements from individual particles rather than time consuming Raman mapping. For correlative Raman-electron microscope imaging, the coordinates of the particles on the filter are marked (at the Raman instrument), and then located again with the SEM. The size of the two smallest identified plastics in the presented frame were 1092 nm x 780 nm and 936 nm x 640 nm for particles 1 and 2, respectively (the measured distances are marked in Supporting Information Figure S5).

While we can identify individual particles, we also notice the presence of particle clusters or aggregates. Obviously, the clusters complicate Raman spectrum acquisition as we operate at the limit of the optical resolution of the Raman microscope. SEM combined with EDS was used to provide further verification of particle composition. According to the EDS maps, particle 1 in Figure 7 is confirmed to be carbon, which, along with the Raman spectra provided in Supporting Information Figure S6, indicates that it is plastic. The size of it is 786 nm x 462 nm. In fact, it appears that the plastic particle itself is a cluster

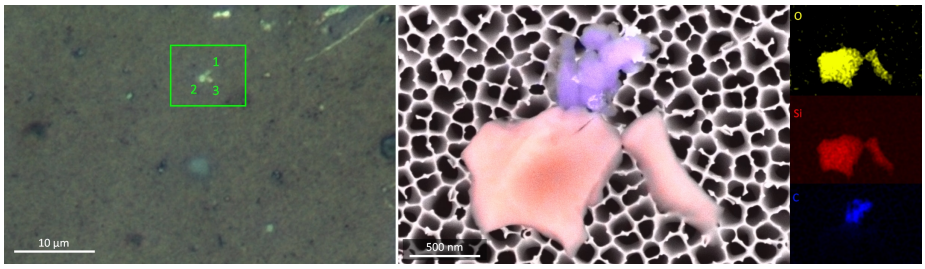

Figure 7: A cluster of three particles imaged with optical microscope (left), and with both overlaid and individual element maps (right).

of four or more smaller plastic particles. Particles 2 and 3 are made of silicon and oxygen suggesting they are sand (SiO_2). The particles other than plastic still present in the sample after purification are discussed in detail later in the text.

Many of the current nanoplastic extraction protocols presented in the literature rely on minimal sample preparation prior analysis limiting the sample size to a drop due to disturbances caused by the organic and inorganic matter in the sample. The Raman tweezers[26] technique can detect nanoplastic particles from 10 µl of seawater cast between two microscope slides, however, no electron microscope images can be correlated with the detected particles due to the encapsulation.

In fact, only a few works that demonstrate SEM imaging of nanoplastics from within environmental samples exist. Aggregating several nanoplastic particles into a cluster together with silver nanoparticles to create the SERS-effect has been suggested. Electron microscope images from the clusters were successfully provided.[28,44] Chang et al.[27] were able to find single particles rather than clusters using Raman mapping and subsequently imaging them with SEM. However, their sample size was, as well, limited to 10 µl and the difficulty of analyzing an environmental sample was acknowledged. Xu et al.[30] were able to detect nanoplastic particles from air samples which they had digested in H_2O_2. They could image individual particles using correlative Raman and electron microscopy. However, as we have demonstrated, seawater is more complicated matrix than air and thus requires further purification and filtration steps. Therefore, as far as we know, we propose the first method to detect nanoplastic particles microscopically from seawater from a substantially larger sample size (1 liter) than previously demonstrated (10 µl).

The main shortcomings of the method, as already pointed out, include occasional identification of particles other than plastic and the formation of aggregates, small or large. Figure 8 shows element maps of two aggregates present in the sample obtained using the EDS (the spectra measured at locations 1–4 are given in the Supporting Information Figure S7). Carbon in the maps is marked with blue and thus is the polystyrene. The spectrum collected at location (3) indicates the presence of mainly C. The composition of the particles similar to

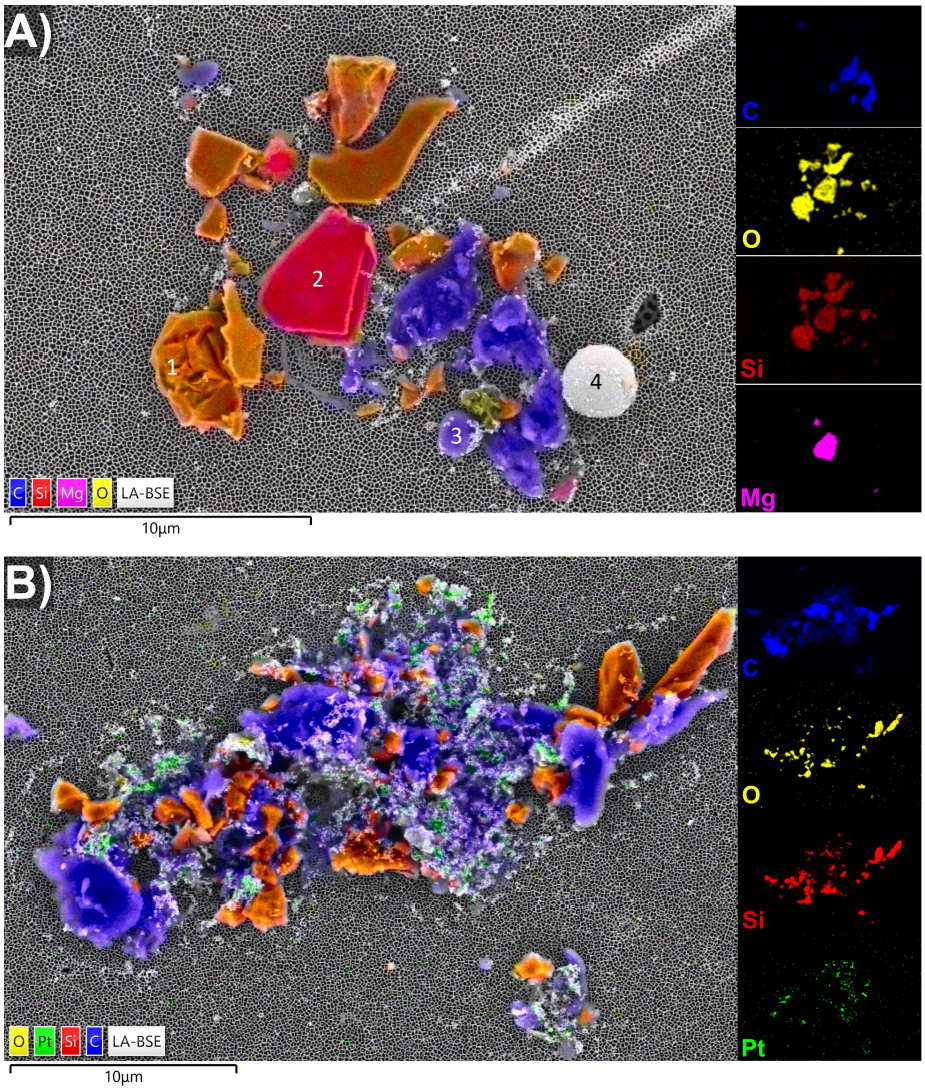

Figure 8: Two examples of clusters detected in the sample after purification. Plastics are marked with blue (carbon), sand and clay are marked with orange (Si, O, Na) and red (Si, O, Mg). Platinum is marked with green.

locations 1 and 2 appears to be silicon oxides with Na and Mg, corresponding to beach sand and clay from the sample collection site. Some Pt-coated spherical aluminium oxide particles were also observed, as indicated by the spectrum obtained from location (4), suggesting their presence on the filter disc before the Pt coating. Figure 8B shows another type of contaminant with same composition as at location 4, which are the small granular clusters colored with green

(Pt) in the map. They as well are present on the filter surface fresh from the pack (for images see Supporting Information Figure S8). In SERS activation, the clusters are coated with Pt, and apparently breaking off from the filter disc and aggregating with the plastic and sand particles during the filtration process.

In the herein described purification method the water samples were let to settle (in dark and at 3 °C) during which time most of the sand precipitated on the bottom of the flask. It appears that this wasn't sufficient to remove all the sand. We know from microplastic literature that density separation using heavy liquids can be used to remove sand and other sediment material from samples.[45] Because of the colloidal nature of nanoplastics, density separation methods are more challenging to apply, but possible if centrifugation is used.[46] Another way to remedy the issue would be to collect samples from deeper waters further away from the shore where there is less sand mixed with the water. Thus addition of heavy liquid separation or any other additional purification steps should be considered depending on the water type at the sample collection site.

Despite the limitations, as we have demonstrated, nanoplastic particles can be detected to a reasonable degree from seawater samples. To quantify the efficacy of our process we measured its particle recovery rate i.e. how many percent of added test particles can be recovered after the processing. To establish a universally applicable reference that is both replicable and enables reliable comparisons with other methods, we determined the recovery rate of the process using ultrapure water (Milli-Q) instead of environmental water. Environmental water sources will exhibit variations based on factors such as type (seawater, lake, river, etc.), time of the year, and location. Recovery rates in environmental water are expected to fall below that of what is measured in ultrapure water due to more complicated medium.

To calculate the recovery rate, minimum and maximum dimension of a plastic particle was measured (see Supporting Information Figure S2 for an example image), and the recovery rate is thus reported as a function of both dimensions. The results are presented in Figure 9. The average efficiency for particles having maximum dimension between 200-1000 nm is 5.5 %. No smaller than 200 nm particles are recovered as the filter pore size was 200 nm. The average recovery rate for particles having their minimum dimension between 100 – 1000 nm is 8.6 %. A clear general trend is observed, where larger particles are recovered more efficiently than smaller ones.

Recovery rates for nanoplastics analyzed using *mass-spectrometry* based method range from 12.7 up to 100 %.[47] Surprisingly, we found no previous literature for comparing our recovery rates calculated from microscope images. That said, Hu et al.[44] reported a recovery rate of 87.5–110%, contrasting significantly with our results. Unfortunately, they did not provide a description of how the values were measured, making a proper evaluation between the methods difficult.

While we targeted nanoplastics in this study, the microplastic collection efficiency was determined as well. Again, similar trend as for nanoplastics was observed. The average recovery rate for plastics being at most 1-10 µm in dimension was 36.6 %, and when calculated according to the minimum dimension

we got 47.8 %. Tabulated values for recovery rates plotted in Figure 9 are given in Supporting Information Table S1 and S2. In comparison with prior studies, Du et al.[48] reported a 7 % recovery rate for small microplastics in the 1 – 20 µm range. Our study clearly exceeds this reported rate. In fact, it appears that our recovery rate at around 10 µm approaches that what is typically reported for microplastics (< 5 mm) in water, which according to a recent review is on average 82 % for low density polymers such as PS.[49]

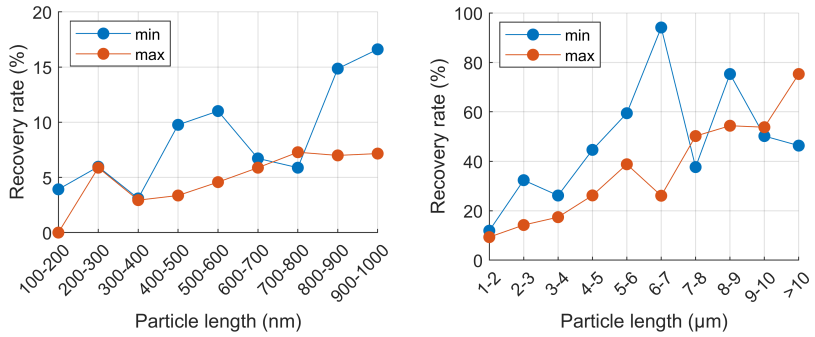

Figure 9: Recovery rates for nanoplastics (left) and microplastics (right). Two graphs are shown per figure: one as a function of particle's largest dimension (max), and the other as a function of its smallest dimension (min).

Background contamination of our laboratory and the contamination arising from the process itself was monitored during the test period. Level of contamination was measured by calculating particles from a control sample which was 1 liter of ultrapure water (Milli-Q) processed with the method described in this paper. The most notable type of contamination is polycarbonate particles which we expect to arise from the polycarbonate filters that were used. The PC contamination was 123 particles / 1 mm^2, which is 10 times smaller than the recovered PS concentration (1082/mm^2). Moreover, PC doesn't belong in the most common plastics, thus its presence doesn't hamper the environmental analyses that target the PP, PET, PE. Other plastics in the laboratory equipment used in the process were teflon (filter grid holder and the support grid for the filters) and PP (support ring around Al_2O_3 filters), however teflon and PP were not detected in control samples.

Contamination not relating to the process but expected to be our laboratory specific were cellulose[50] (most likely from paper wipes), graphite[51] and the blue pigment copper phthalocyanine[52] based on their Raman spectra (given in Supporting Information Figure S9). As they are not plastics, their presence doesn't hamper the plastic analyses. Each laboratory is expected to have their own specific background contamination, and obviously efforts should be made to minimize it. Fortunately, as long as the contamination does not involve plastic, it does not significantly impede the analyses, except for the additional time required to measure extra particles.

4 Conclusions

In this work we presented a method which would allow the identification and production of high magnification images of nanoplastics from 1 liter of seawater using Raman and electron microscopy. We conclude that we have succeeded to increase the sample size from the common sample of some microliters up to one liter of actual seawater. How much water is enough to make a reliable nanoplastic analysis is yet to be determined. However, these results should open up new possibilities for researchers, and pave the way towards accurate analytical protocol for nanoplastic detection.

5 Acknowledgments

We thank the Weisell-foundation for funding. The study has utilized research infrastructure facilities provided by FINMARI (the Finnish Marine Research Infrastructure consortium). The study contributes to the thematic collaboration of The Sea and Maritime Studies according to the strategy of Turku University.

References

[1] Roland Geyer, Jenna R Jambeck, and Kara Lavender Law. Production, use, and fate of all plastics ever made. *Science advances*, 3(7):e1700782, 2017.

[2] Edward J Carpenter and KL Smith Jr. Plastics on the sargasso sea surface. *Science*, 175(4027):1240–1241, 1972.

[3] EL Venrick, TW Backman, WC Bartram, CJ Platt, MS Thornhill, and RE Yates. Man-made objects on the surface of the central north pacific ocean. *Nature*, 241(5387):271–271, 1973.

[4] Amanda L Dawson, So Kawaguchi, Catherine K King, Kathy A Townsend, Robert King, Wilhelmina M Huston, and Susan M Bengtson Nash. Turning microplastics into nanoplastics through digestive fragmentation by antarctic krill. *Nature communications*, 9(1):1001, 2018.

[5] Natalia P Ivleva, Alexandra C Wiesheu, and Reinhard Niessner. Microplastic in aquatic ecosystems. *Angewandte Chemie International Edition*, 56(7):1720–1739, 2017.

[6] Julien Gigault, Boris Pedrono, Benoît Maxit, and Alexandra Ter Halle. Marine plastic litter: the unanalyzed nano-fraction. *Environmental science: nano*, 3(2):346–350, 2016.

[7] Laura M Hernandez, Joel Grant, Parvin Shakeri Fard, Jeffrey M Farner, and Nathalie Tufenkji. Analysis of ultraviolet and thermal degradations of four common microplastics and evidence of nanoparticle release. *Journal of Hazardous Materials Letters*, 4:100078, 2023.

[8] Laura M Hernandez, Elvis Genbo Xu, Hans CE Larsson, Rui Tahara, Vimal B Maisuria, and Nathalie Tufenkji. Plastic teabags release billions of microparticles and nanoparticles into tea. *Environmental science & technology*, 53(21):12300–12310, 2019.

[9] Dunzhu Li, Yunhong Shi, Luming Yang, Liwen Xiao, Daniel K Kehoe, Yurii K Gun'ko, John J Boland, and Jing Jing Wang. Microplastic release from the degradation of polypropylene feeding bottles during infant formula preparation. *Nature Food*, 1(11):746–754, 2020.

[10] Janice Brahney, Margaret Hallerud, Eric Heim, Maura Hahnenberger, and Suja Sukumaran. Plastic rain in protected areas of the united states. *Science*, 368(6496):1257–1260, 2020.

[11] Aurélie Wahl, Corentin Le Juge, Mélanie Davranche, Hind El Hadri, Bruno Grassl, Stephanie Reynaud, and Julien Gigault. Nanoplastic occurrence in a soil amended with plastic debris. *Chemosphere*, 262:127784, 2021.

[12] Melanie Bergmann, Sophia Mützel, Sebastian Primpke, Mine B Tekman, Jürg Trachsel, and Gunnar Gerdts. White and wonderful? microplastics prevail in snow from the alps to the arctic. *Science advances*, 5(8):eaax1157, 2019.

[13] Dušan Materić, Anne Kasper-Giebl, Daniela Kau, Marnick Anten, Marion Greilinger, Elke Ludewig, Erik van Sebille, Thomas Röckmann, and Rupert Holzinger. Micro-and nanoplastics in alpine snow: a new method for chemical identification and (semi) quantification in the nanogram range. *Environmental science & technology*, 54(4):2353–2359, 2020.

[14] Inta Dimante-Deimantovica, Saija Saarni, Marta Barone, Natalja Buhhalko, Normunds Stivrins, Natalija Suhareva, Wojciech Tylmann, Alvise Vianello, and Jes Vollertsen. Downward migrating microplastics in lake sediments are a tricky indicator for the onset of the anthropocene. *Science advances*, 10(8):eadi8136, 2024.

[15] XiaoZhi Lim et al. Microplastics are everywhere—but are they harmful. *Nature*, 593(7857):22–25, 2021.

[16] Antonio Ragusa, Alessandro Svelato, Criselda Santacroce, Piera Catalano, Valentina Notarstefano, Oliana Carnevali, Fabrizio Papa, Mauro Ciro Antonio Rongioletti, Federico Baiocco, Simonetta Draghi, et al. Plasticenta: First evidence of microplastics in human placenta. *Environment international*, 146:106274, 2021.

[17] Heather A Leslie, Martin Jm Van Velzen, Sicco H Brandsma, A Dick Vethaak, Juan J Garcia-Vallejo, and Marja H Lamoree. Discovery and quantification of plastic particle pollution in human blood. *Environment international*, 163:107199, 2022.

[18] Laurens DB Mandemaker and Florian Meirer. Spectro-microscopic techniques for studying nanoplastics in the environment and in organisms. *Angewandte Chemie International Edition*, 62(2):e202210494, 2023.

[19] Wiwik Bauten, Maximilian Nöth, Tetiana Kurkina, Francisca Contreras, Yu Ji, Cloé Desmet, Miguel Ángel Serra, Douglas Gilliland, and Ulrich Schwaneberg. Plastibodies for multiplexed detection and sorting of microplastic particles in high-throughput. *Science of The Total Environment*, 860:160450, 2023.

[20] Anna Winkler, Francesco Fumagalli, Claudia Cella, Douglas Gilliland, Paolo Tremolada, and Andrea Valsesia. Detection and formation mechanisms of secondary nanoplastic released from drinking water bottles. *Water Research*, 222:118848, 2022.

[21] Christian Schwaferts, Vanessa Sogne, Roland Welz, Florian Meier, Thorsten Klein, Reinhard Niessner, Martin Elsner, and Natalia P. Ivleva. Nanoplastic analysis by online coupling of raman microscopy and field-flow fractionation enabled by optical tweezers. *Analytical Chemistry*, 92(8):5813–5820, 2020. PMID: 32073259.

[22] Wen Zhang, Zhiqiang Dong, Ling Zhu, Yuanzhang Hou, and Yuping Qiu. Direct observation of the release of nanoplastics from commercially recycled

plastics with correlative raman imaging and scanning electron microscopy. *ACS Nano*, 14(7):7920–7926, 2020. PMID: 32441911.

[23] Zahra Sobhani, Xian Zhang, Christopher Gibson, Ravi Naidu, Mallavarapu Megharaj, and Cheng Fang. Identification and visualisation of microplastics/nanoplastics by raman imaging (i): Down to 100 nm. *Water Research*, 174:115658, 2020.

[24] Hanjin Yoo, Hayeong Lee, Changmin Park, Dongha Shin, and Chul-Un Ro. Novel single-particle analytical technique for submicron atmospheric aerosols: Combined use of dark-field scattering and surface-enhanced raman spectroscopy. *Analytical Chemistry*, 94(38):13028–13035, 2022. PMID: 36107822.

[25] Tong Yang, Jialuo Luo, and Bernd Nowack. Characterization of nanoplastics, fibrils, and microplastics released during washing and abrasion of polyester textiles. *Environmental Science & Technology*, 55(23):15873–15881, 2021. PMID: 34784483.

[26] Raymond Gillibert, Gireeshkumar Balakrishnan, Quentin Deshoules, Morgan Tardivel, Alessandro Magazzù, Maria Grazia Donato, Onofrio M. Maragò, Marc Lamy de La Chapelle, Florent Colas, Fabienne Lagarde, and Pietro G. Gucciardi. Raman tweezers for small microplastics and nanoplastics identification in seawater. *Environmental Science & Technology*, 53(15):9003–9013, 2019. PMID: 31259538.

[27] Lin Chang, Shan Jiang, Jie Luo, Jianfa Zhang, Xiaohong Liu, Chong-Yew Lee, and Wei Zhang. Nanowell-enhanced raman spectroscopy enables the visualization and quantification of nanoplastics in the environment. *Environmental Science: Nano*, 9(2):542–553, 2022.

[28] Lulu Lv, Lei He, Shiqi Jiang, Jinjun Chen, Chunxia Zhou, Junhao Qu, Yuqin Lu, Pengzhi Hong, Shengli Sun, and Chengyong Li. In situ surface-enhanced raman spectroscopy for detecting microplastics and nanoplastics in aquatic environments. *Science of the Total Environment*, 728:138449, 2020.

[29] Rui Hu, Kaining Zhang, Wei Wang, Long Wei, and Yongchao Lai. Quantitative and sensitive analysis of polystyrene nanoplastics down to 50 nm by surface-enhanced raman spectroscopy in water. *Journal of Hazardous Materials*, 429:128388, 2022.

[30] Guanjun Xu, Hanyun Cheng, Robin Jones, Yiqing Feng, Kedong Gong, Kejian Li, Xiaozhong Fang, Muhammad Ali Tahir, Ventsislav Kolev Valev, and Liwu Zhang. Surface-enhanced raman spectroscopy facilitates the detection of microplastics <1 um in the environment. *Environmental Science & Technology*, 54(24):15594–15603, 2020. PMID: 33095569.

[31] Ruth Schmidt, Manfred Nachtnebel, Martina Dienstleder, Sabrina Mertschnigg, Hartmuth Schroettner, Armin Zankel, Michael Poteser, Hans-Peter Hutter, Wolfgang Eppel, and Harald Fitzek. Correlative sem-raman mi-

croscopy to reveal nanoplastics in complex environments. *Micron*, 144:103034, 2021.

[32] Paul L. Stiles, Jon A. Dieringer, Nilam C. Shah, and Richard P. Van Duyne. Surface-enhanced raman spectroscopy. *Annual Review of Analytical Chemistry*, 1(1):601–626, 2008. PMID: 20636091.

[33] Hind El Hadri, Julien Gigault, Benoit Maxit, Bruno Grassl, and Stéphanie Reynaud. Nanoplastic from mechanically degraded primary and secondary microplastics for environmental assessments. *NanoImpact*, 17:100206, 2020.

[34] Felix Pfeiffer and Elke Kerstin Fischer. Various digestion protocols within microplastic sample processing—evaluating the resistance of different synthetic polymers and the efficiency of biogenic organic matter destruction. *Frontiers in Environmental Science*, 8:572424, 2020.

[35] Mohammed SM Al-Azzawi, Simone Kefer, Jana Weißer, Julia Reichel, Christoph Schwaller, Karl Glas, Oliver Knoop, and Jörg E Drewes. Validation of sample preparation methods for microplastic analysis in wastewater matrices—reproducibility and standardization. *Water*, 12(9):2445, 2020.

[36] Alexandra M Gulizia, Eve Brodie, Renee Daumuller, Sarah B Bloom, Tayla Corbett, Marina MF Santana, Cherie A Motti, and George Vamvounis. Evaluating the effect of chemical digestion treatments on polystyrene microplastics: Recommended updates to chemical digestion protocols. *Macromolecular Chemistry and Physics*, 223(13):2100485, 2022.

[37] Hermann Ehrlich, Konstantinos D Demadis, Oleg S Pokrovsky, and Petros G Koutsoukos. Modern views on desilicification: biosilica and abiotic silica dissolution in natural and artificial environments. *Chemical reviews*, 110(8):4656–4689, 2010.

[38] Martin G. J. Löder, Hannes K. Imhof, Maike Ladehoff, Lena A. Löschel, Claudia Lorenz, Svenja Mintenig, Sarah Piehl, Sebastian Primpke, Isabella Schrank, Christian Laforsch, and Gunnar Gerdts. Enzymatic purification of microplastics in environmental samples. *Environmental Science & Technology*, 51(24):14283–14292, 2017. PMID: 29110472.

[39] Bhavya Sharma, Renee R Frontiera, Anne-Isabelle Henry, Emilie Ringe, and Richard P Van Duyne. Sers: Materials, applications, and the future. *Materials today*, 15(1-2):16–25, 2012.

[40] Qing Yang, Shaoying Zhang, Jie Su, Shu Li, Xiaochen Lv, Jing Chen, Yongchao Lai, and Jinhua Zhan. Identification of trace polystyrene nanoplastics down to 50 nm by the hyphenated method of filtration and surface-enhanced raman spectroscopy based on silver nanowire membranes. *Environmental Science & Technology*, 56(15):10818–10828, 2022.

[41] Barbara E Oßmann, George Sarau, Sebastian W Schmitt, Heinrich Holtmannspötter, Silke H Christiansen, and Wilhelm Dicke. Development of an optimal filter substrate for the identification of small microplastic particles in food by micro-raman spectroscopy. *Analytical and bioanalytical chemistry*, 409:4099–4109, 2017.

[42] Dušan Materić, Rupert Holzinger, and Helge Niemann. Nanoplastics and ultrafine microplastic in the dutch wadden sea – the hidden plastics debris? *Science of The Total Environment*, 846:157371, 2022.

[43] Dušan Materić, Mike Peacock, Joshua Dean, Martyn Futter, Trofim Maximov, Filip Moldan, Thomas Röckmann, and Rupert Holzinger. Presence of nanoplastics in rural and remote surface waters. *Environmental Research Letters*, 17(5):054036, 2022.

[44] Rui Hu, Kaining Zhang, Wei Wang, Long Wei, and Yongchao Lai. Quantitative and sensitive analysis of polystyrene nanoplastics down to 50 nm by surface-enhanced raman spectroscopy in water. *Journal of Hazardous Materials*, 429:128388, 2022.

[45] Saija Saarni, Samuel Hartikainen, Senja Meronen, Emilia Uurasjärvi, Maarit Kalliokoski, and Arto Koistinen. Sediment trapping–an attempt to monitor temporal variation of microplastic flux rates in aquatic systems. *Environmental Pollution*, 274:116568, 2021.

[46] Caterina Minelli, Aneta Sikora, Raul Garcia-Diez, Katia Sparnacci, Christian Gollwitzer, Michael Krumrey, and Alex G Shard. Measuring the size and density of nanoparticles by centrifugal sedimentation and flotation. *Analytical Methods*, 10(15):1725–1732, 2018.

[47] Huiwen Cai, Elvis Genbo Xu, Fangni Du, Ruilong Li, Jingfu Liu, and Huahong Shi. Analysis of environmental nanoplastics: Progress and challenges. *Chemical Engineering Journal*, 410:128208, 2021.

[48] Fangni Du, Huiwen Cai, Lei Su, Wei Wang, Liwu Zhang, Chengjun Sun, Beizhan Yan, and Huahong Shi. The missing small microplastics: easily generated from weathered plastic pieces in labs but hardly detected in natural environments. *Environmental Science: Advances*, 2024.

[49] Chloe Way, Malcolm D Hudson, Ian D Williams, and G John Langley. Evidence of underestimation in microplastic research: a meta-analysis of recovery rate studies. *Science of the Total Environment*, 805:150227, 2022.

[50] Ana Paula P Alves, Luana PZ de Oliveira, Aloísio AN Castro, Reiner Neumann, Luiz FC de Oliveira, Howell GM Edwards, and Antonio C Sant'Ana. The structure of different cellulosic fibres characterized by raman spectroscopy. *Vibrational Spectroscopy*, 86:324–330, 2016.

[51] Andrea C Ferrari. Raman spectroscopy of graphene and graphite: Disorder, electron–phonon coupling, doping and nonadiabatic effects. *Solid state communications*, 143(1-2):47–57, 2007.

[52] Taoyu Zou, Jiawei Chang, Qiuyuan Chen, Zhifeng Nie, Liangfei Duan, Tingting Guo, Yumin Song, Wei Wu, and Hai Wang. Novel strategy for organic cocrystals of n-type and p-type organic semiconductors with advanced optoelectronic properties. *ACS omega*, 5(21):12067–12072, 2020.